2009

Identification of antigen-presenting dendritic cells in mouse aorta and cardiac valves

Jae-hoon Choi

Yoonkyung Do

Cheolho Cheong

Identification of antigen–presenting dendritic cells in mouse aorta and cardiac valves

Jae-Hoon Choi,[1,4] Yoonkyung Do,[1,4] Cheolho Cheong,[1,4] Hyein Koh,[1,4] Silvia B. Boscardin,[2] Yong-Seok Oh,[3] Leonia Bozzacco,[1,4] Christine Trumpfheller,[1,4] Chae Gyu Park,[1,4] and Ralph M. Steinman[1,4]

[1]Laboratory of Cellular Physiology and Immunology, [2]Laboratory of Molecular Immunology, [3]Laboratory of Molecular and Cellular Neuroscience, and [4]Chris Browne Center for Immunology, The Rockefeller University, New York, NY 10065

Presumptive dendritic cells (DCs) bearing the CD11c integrin and other markers have previously been identified in normal mouse and human aorta. We used CD11c promoter–enhanced yellow fluorescent protein (EYFP) transgenic mice to visualize aortic DCs and study their antigen–presenting capacity. Stellate EYFP+ cells were readily identified in the aorta and could be double labeled with antibodies to CD11c and antigen–presenting major histocompatability complex (MHC) II products. The DCs proved to be particularly abundant in the cardiac valves and aortic sinus. In all aortic locations, the CD11c+ cells localized to the subintimal space with occasional processes probing the vascular lumen. Aortic DCs expressed little CD40 but expressed low levels of CD1d, CD80, and CD86. In studies of antigen presentation, DCs selected on the basis of EYFP expression or binding of anti–CD11c antibody were as effective as DCs similarly selected from the spleen. In particular, the aortic DCs could cross–present two different protein antigens on MHC class I to CD8+ TCR transgenic T cells. In addition, after intravenous injection, aortic DCs could capture anti–CD11c antibody and cross–present ovalbumin to T cells. These results indicate that bona fide DCs are a constituent of the normal aorta and cardiac valves.

The Journal of Experimental Medicine

CORRESPONDENCE
Ralph M. Steinman:
steinma@mail.rockefeller.edu
OR
Chae Gyu Park:
parkc@mail.rockefeller.edu

Inflammation is a component of many vascular disorders such as aortic aneurysm, giant cell arteritis, Takayasu's disease, and atherosclerosis (1–4). DCs carry out many innate responses and orchestrate adaptive immunity (5). It is therefore important to assess the presence and properties of DCs in major blood vessels.

Initially, electron microscopy and labeling for several intracellular markers were used to demonstrate DCs in human aorta, primarily in a subendothelial location (6–9). Ma-Krupa et al. (10) and Pryshchep et al. (11) then used more cell-restricted markers to identify DCs in increased numbers in human arteries, whereas Bobryshev (12) reported increased numbers of cells expressing S100, CD1a, and p55 markers in the intima and adventitia during atherosclerosis. Cells bearing the CD11c integrin, which is characteristically expressed at high levels on DCs, were also identified in the normal aortic intima and in atherosclerosis-prone areas in mice (13, 14). The numbers of aortic CD11c+ cells increased with aging and atherosclerosis through a recruitment process involving

CX3CR1 chemokine receptor and VCAM-1 (13, 15, 16).

Although abundant CD11c expression is a well-known marker for DCs, other cell types can express moderate levels of CD11c, including activated NK cells, some macrophages, and even some T cells (17–21). Therefore, additional criteria are required to identify DCs in the vascular wall in the steady state and ultimately disease, particularly the capacity of DCs to express MHC class II and present antigens to T lymphocytes.

In this study, we found that the CD11c promoter–enhanced yellow fluorescent protein (EYFP) transgenic mouse developed by Lindquist et al. (22) is valuable to identify and study CD11c+ cells from the normal mouse aorta. We will report on the location, cell surface markers, and antigen-presenting functions of DCs and also describe their abundance in all of the cardiac valves.

RESULTS AND DISCUSSION
Aortic DCs are readily visualized in CD11c–EYFP transgenic mice

The CD11c–EYFP transgenic mouse (C57BL/6 background), in which expression of the EYFP gene is controlled by the CD11c promoter, was developed to better visualize and characterize DCs in situ, beginning with lymphoid organs in the steady state (22). We performed flow cytometry on aortic cell suspensions and found that 0.25–0.5% of the cells expressed EYFP, with the signal ranging from low to high (Fig. 1 A). The isolated EYFP+ cells also could be stained for cell surface CD11c and MHC class II (Fig. 1 B, top). If we isolated CD11c+ cells from normal nontransgenic C57BL/6 mice, we again saw clear labeling for MHC class II (Fig. 1 B, bottom), but the signals with anti-CD11c were much weaker than those observed with EYFP mice. When we examined whole mounts of the aorta, brightly EYFP+ dendritic profiles were evident, and these could be double labeled with antibodies to CD11c and MHC class II (Fig. 1 C), two markers of typical DCs in the steady state. However this staining required the use of tyramide amplification (see Materials and methods). These results indicate that the CD11c-EYFP transgenic mouse is valuable to identify and visualize aortic DCs in cell suspensions and in situ.

### Aortic DCs are abundant in the aortic valve and sinus

To examine the distribution of DCs in the aorta, we examined sheet preparations by confocal microscopy. In accordance with previous reports (13, 15), we found that the EYFP+ DCs were primarily in the intima and in focal accumulations, i.e., in the lesser curvature of the aortic arch and the openings of arteries, rather than a scattered distribution in the adventitia (Fig. 2 A).

When we turned to the root of the aorta, as diagrammed in Fig. 2 B, large numbers of DCs were found in the aortic valve and sinus (Fig. 2 C). We then prepared cell suspensions from the aortic valve and sinus and compared the yield of DCs relative to suspensions from the aortic arch and descending aorta. The aortic root, i.e., valve and sinus, suspensions had more numerous EYFP cells (Fig. 2 D, top), confirming the observations in intact tissue (Fig. 2 C). Likewise when we studied nontransgenic C57BL/6 mice and stained cell suspensions with anti-CD11c antibody, the aortic root had more abundant DCs, although the intensity of the anti-CD11c signal was much reduced relative to the EYFP signal in transgenic mice (Fig. 2 D). Mean values for three experiments are shown in Fig. 2 D (bottom).

The presence of DCs in normal aortic valve prompted us to examine other normal cardiac valves. Accumulations of DCs have been reported in valves in degenerative disease, bioprostheses, and papillary fibroelastomas (23, 24). In a single prior study of normal aortic valves, fresh and cryopreserved tissue had no DCs (25). However, we observed many EYFP+ DCs in the left (mitral) and right (tricuspid) atrioventricular valves (Fig. 2 E). These findings with CD11c-EYFP mice extend prior studies by showing that aortic DCs are especially abundant in the root of the aorta and all cardiac valves.

Aortic DCs are mainly localized in the subintimal space

To examine the position of the EYFP+ DCs in the aortic wall, we performed confocal microscopy with simultaneous staining for CD31 to mark the vascular endothelium (26). In addition, the confocal images were reconstituted into three-dimensional images using the Imaris program to gain better understanding of the anatomical localization of aortic DCs. The DCs were
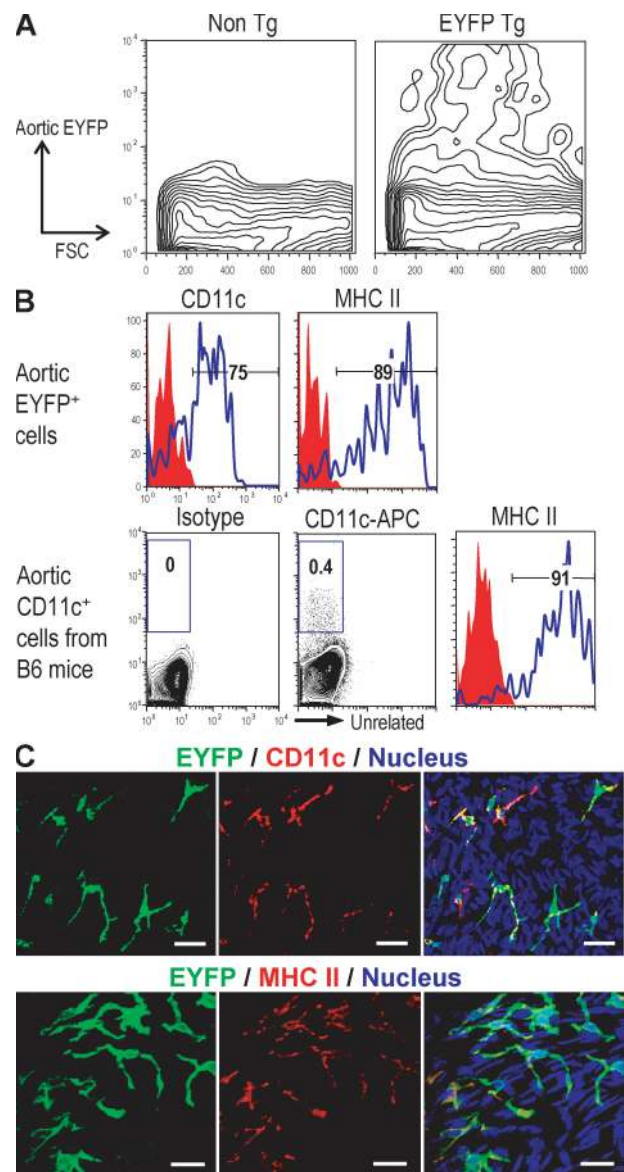

Figure 1. Visualizing aortic DCs using CD11c–EYFP transgenic mice. (A) The presence of EYFP+ cells in aortic cell suspension from EYFP transgenic mice. Aortic segments from EYFP transgenic mice (*n* = 5) were pooled and dissociated by incubation with an enzyme mixture (see Materials and methods) and then subjected to flow cytometric analysis. (B) Experiments were performed as in A, but the aortic CD11c+ cells were from nontransgenic mice (*n* = 3) and compared for expression of CD11c and MHC II to aortic EYFP+ cells. (C) Immunohistochemical staining of CD11c and MHC II in aortic sheets. Each experiment was performed at least three times. Bars, 20 μm.

localized beneath the endothelium (Fig. 3, A and B; and Video 1, available at http://www.jem.org/cgi/content/full/jem .20082129/DC1), although infrequently in the aortic sinus, dendritic processes penetrated between endothelial cells into the lumen (Fig. 3 A, middle, arrow; and Video 2). In all sites, i.e., aortic root, aortic arch, and descending aorta, the bodies of the CD11c+ DCs were located in the subintimal space, and most of the dendritic processes extended laterally within the subintimal areas (Fig. 3, A and B, red).

In previous studies, it has been shown that intestinal DCs extend their dendritic processes across the epithelium to capture bacteria in lumen (27). To determine whether aortic DCs could extend processes into the vessel lumen and capture proteins, we applied anti-CD11c antibody to whole segments of aorta from CD11c-EYFP mice, i.e., without tissue permeabilization using Triton X-100. Parts of some of the DCs were stained with anti-CD11c antibody (Fig. 3 C). Next, we injected anti-CD11c antibody i.v. to CD11c-EYFP mice and
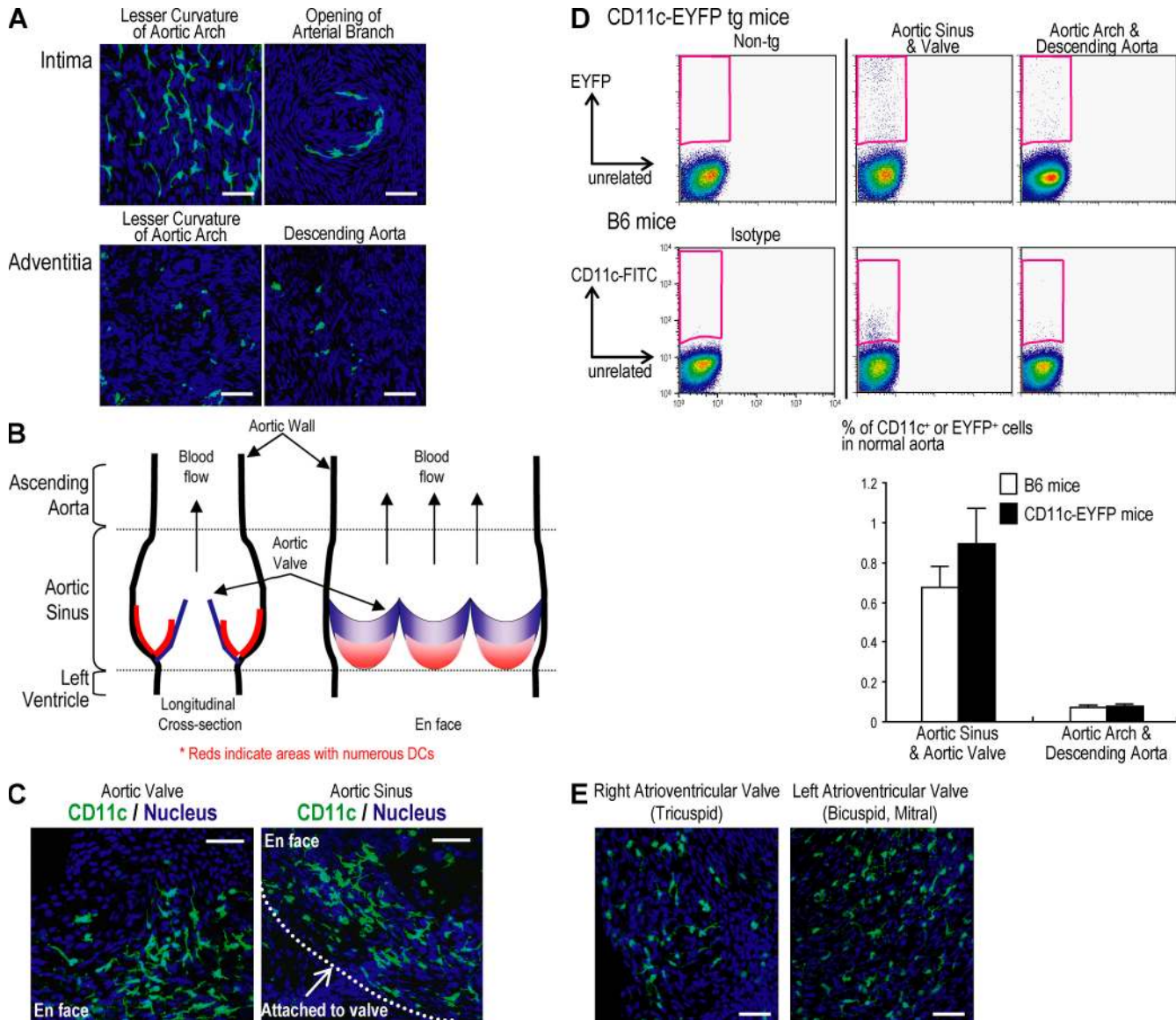
Figure 2. **Predominant localization of aortic DCs in the aortic valve and sinus.** Aortic segments from aortic sinus to diaphragm were opened longitudinally to make aortic sheets. The distribution of aortic DCs was analyzed using confocal microscopy. (A) EYFP+ DCs in the intima of the aortic arch (top left) and openings of arterial branches (top right). Adventitial EYFP+ DCs were scattered throughout the aorta including aortic arch (bottom left) and descending aorta (bottom right) (B) Diagram of aortic sinus. Red indicates DC-abundant areas. (C) EYFP+ DCs in aortic valve (left) and sinus (right). (D) Flow cytometric analysis of EYFP+ cells. The mean and SD of three experiments are shown below, with the aortic cell suspension in each experiment being from at least three mice. (E) The presence of DCs in normal cardiac valves including left (left panel) and right (right panel) atrioventricular valves. The cardiac valves were isolated using microscissors under guidance of a dissecting microscope. The valvular sheets were mounted on glass slides and observed by confocal microscopy. Each figure is representative of at least three experiments. Bars, 40 µm.
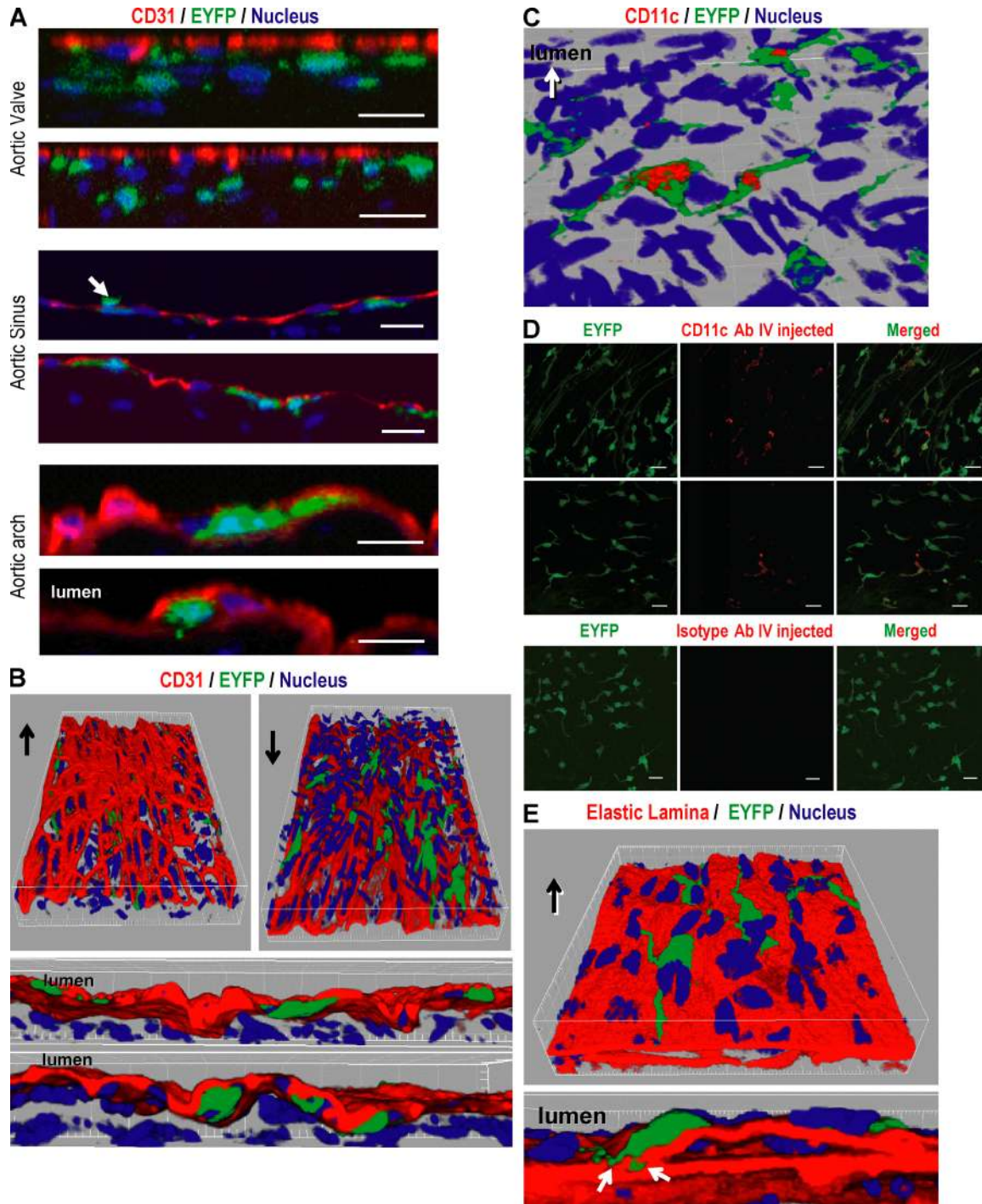
Figure 3. The anatomical position of aortic DCs in aortic wall. After immunostaining the aortic sheet using CD31 antibody to visualize the endothelium, confocal images were taken along the Z axis to visualize all dendritic processes from each EYFP+ DC and were reconstituted to a Z stack. (A) Reconstituted Z planes from aortic valve (top), aortic sinus (middle), and aortic arch (bottom) show that the aortic DCs are localized beneath the endothelium. A small number of DCs in the aortic sinus extend their processes into the vessel lumen (A, middle, arrow). (B) Three-dimensional images were reconstituted using the Imaris program to better visualize the position of aortic DCs. Arrows indicate the vessel lumen side. (C) Exposure of some dendritic processes into the lumen. The aortic sheets from EYFP transgenic mice were stained with CD11c antibody without tissue permeabilization to see whether dendritic processes could capture antibody from the lumen. The confocal images were reconstituted in three dimensions. (D) Biotinylated anti-CD11c and hamster IgG control antibody were injected i.v. to CD11c-EYFP mice. After 3 h, the aortic segments were isolated, incubated with horseradish peroxidase–conjugated streptavidin, and the stained CD11c was enhanced with Alexa Fluor 555 tyramide. (E) The elastic lamina was visualized using its autofluorescence. The confocal images were reconstituted in three dimensions. Each figure is representative of at least three experiments. Bars, 20 μm.

found that some of the DCs were stained by the injected antibody (Fig. 3 D), suggesting exposure of some aortic DC processes to the contents of the lumen.

To investigate whether DC processes extend into the tunica media, the aortic elastic lamina was visualized using its autofluorescence. We found that the DC processes were anchored to the elastic lamina and rarely penetrated the internal elastic lamina (Fig. 3 E and Video 3, available at http://www.jem.org/cgi/content/full/jem.20082129/DC1). These observations indicate a primarily subendothelial location of aortic DCs with some exposure to the blood stream.

## Aortic and splenic DCs have similar but not identical phenotypes

To phenotype aortic DCs, we prepared cell suspensions from aorta and spleen of EYFP transgenic mice and double labeled for CD11c and various markers. Aortic DCs lacked CD40, but expressed low levels of CD1d, CD80, and CD86, indicating their immature status (Fig. 4, top). Splenic EYFP$^+$ DCs had slightly higher amounts of CD1d, CD40, and CD80 when compared with aortic DCs (Fig. 4, bottom). We also analyzed the phenotype of DCs from aorta and spleen of nontransgenic mice and assessed this same panel of markers. Again aortic and spleen DCs were similar in phenotype, with spleen DCs expressing more CD1d, CD40, and CD80, although still not in high amounts (Fig. S1, available at http://www.jem.org/cgi/content/full/jem.20082129/DC1). Together, these findings indicate that aortic DCs are in an immature state with little or no expression of costimulatory molecules.

## Aortic CD11c$^+$ DCs cross–present antigens on MHC class I products

Although there have been several morphological analyses of normal aortic CD11c$^+$ cells, there has been no functional evidence to show that these cells can present antigens to T lymphocytes, including a property that is well developed in some DCs, which is cross-presentation of proteins on MHC class I to CD8$^+$ T cells. To assess this, we first worked out assay conditions for antigen presentation using CD8$^+$ TCR transgenic T cells as reporters for cross-presentation by splenic DCs. As is

evident from Fig. S2 A (available at http://www.jem.org/cgi/content/full/jem.20082129/DC1), splenic DCs presented OVA protein at relatively low doses (60–200 μg/ml) to OT-I transgenic T cells. In contrast, when we studied presentation of the mouse malaria circumsporozoite (CS) protein (CSP) to CSP-specific CD8$^+$ TCR transgenic T cells (YA26), higher concentrations of protein were required than with the OVA-specific OT-I T cells (Fig. S2 B). Likewise, when we used specific peptide as antigen, the OT-1 transgenic T cells were at least 100 times more sensitive than YA26 T cells to antigen in the presence of DCs. All OT-1 cells entered cell cycle in response to 1 pM of peptide, whereas YA26 T cells required 1 nM (Fig. 5 A). With both TCR transgenic T cells, if the DCs were fixed with formaldehyde before testing, presentation of protein antigen, but not preprocessed peptide, was ablated, indicating that our protein preparations were not significantly contaminated with active peptide (Fig. S3, available at http://www.jem.org/cgi/content/full/jem.20082129/DC1). We also assessed the importance of DC dose and time of culture for cross-presentation to CD8$^+$ TCR transgenic T cells. A DC to T cell ratio of 1:6 induced proliferation (two to four cycles of division) in the culture within 3–4 d (Fig. S4). Therefore, OT-I cells are much more sensitive than a T cell clone specific for an important microbial protein and capable of mediating protective anti–mouse malaria immunity in vivo (28).

Using these assay conditions, we first tested aortic CD11c$^+$ cells from normal C57BL/6 (B6) mice (n = 6) isolated on CD11c MACS beads. However, the CD11c-enriched aortic cells only induced weak proliferation of OT-I and OT-II cells (unpublished data). When we enumerated DCs in cells isolated with MACS beads, the DC purity was <10%. To increase the purity of aortic CD11c$^+$ cells, we used CD11c-EYFP transgenic mice. After dissociating the aortic tissue from groups of 10 mice in each experiment, EYFP$^+$ cells were isolated by FACS sorting. From an 8-wk–old adult mouse, we typically isolated ∼1,500 EYFP$^+$ cells from one aortic segment, i.e., from aortic sinus to thoracic aorta inclusive. When the isolated EYFP$^+$ cells were used to present OVA to OT-I and OT-II T cells, we observed strong proliferative responses with most of the T cells entering cell cycle and undergoing several divisions in 4 or 5 d (Fig. 5 B).
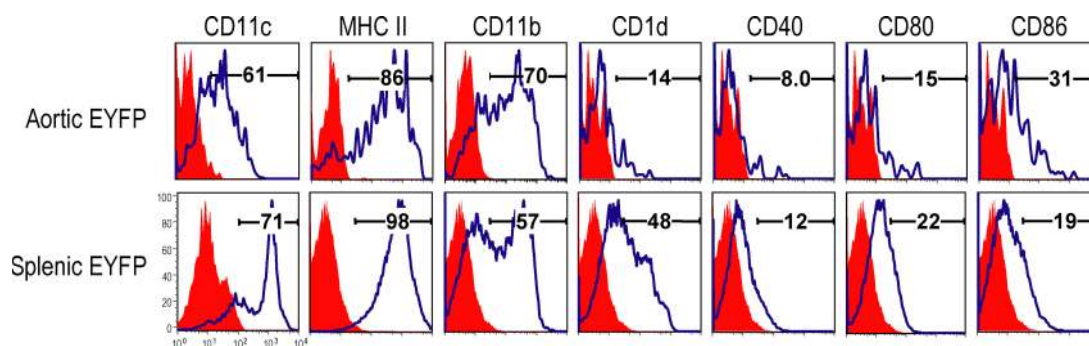
Figure 4. Comparison of cell surface markers of aortic and splenic DCs. Aortic and spleen cell suspensions from transgenic mice (n = 5) was stained with antibodies to each surface marker as shown. Each figure is representative of at least three experiments.
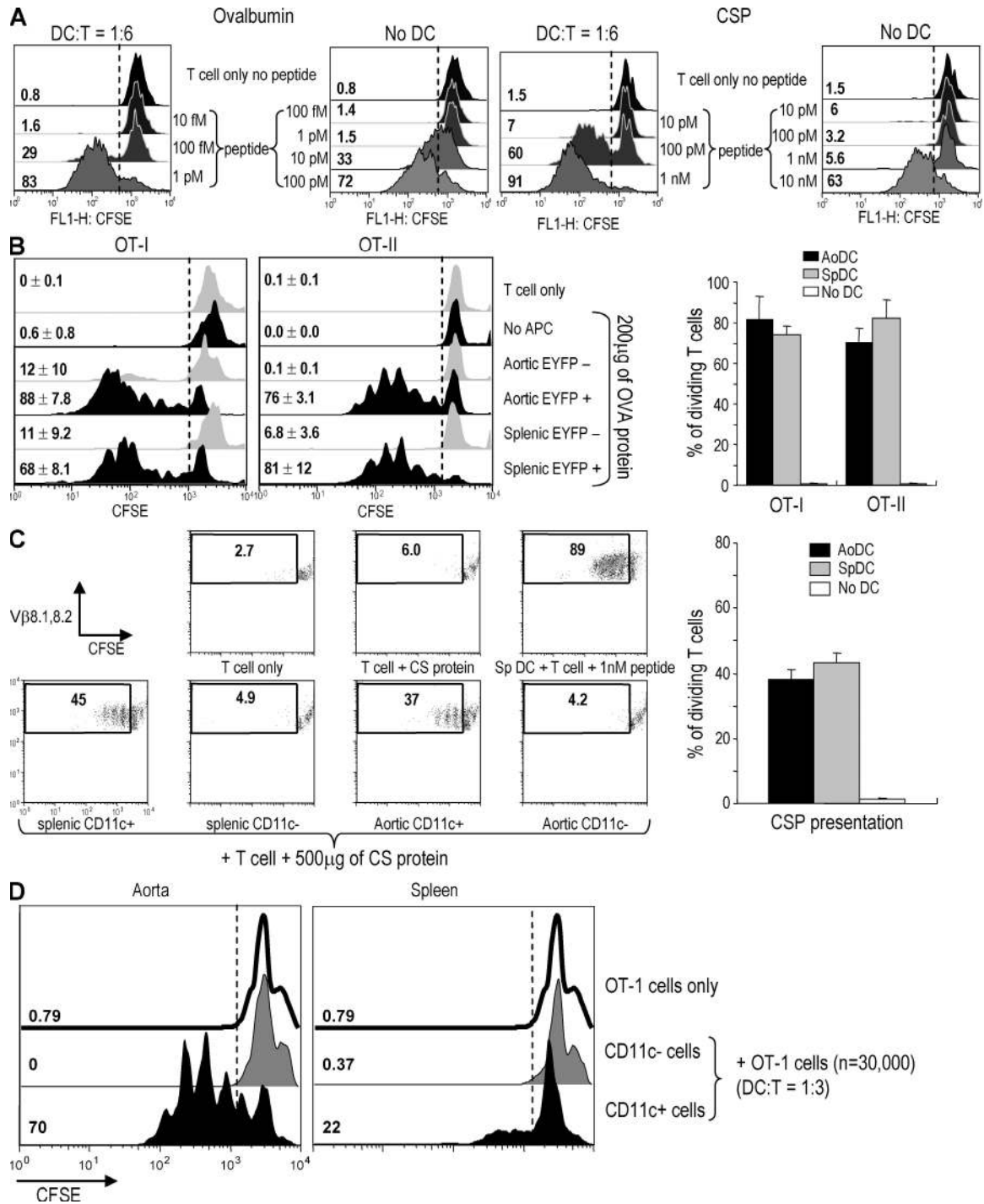
Figure 5. Antigen presentation to T cells by aortic DCs. (A) Comparison between OT-1 and YA26 TCR transgenic CD8+ T cells. The indicated concentrations of OT-1 peptide (SIINFEKL) or CS peptide (SYVPSAEQI) were added to each T cell with or without splenic DCs. After 4 d, T cell proliferation was analyzed by CFSE dilution. (B) Presentation to OVA-specific TCR transgenic T cells. Aortic and splenic EYFP+ and EYFP− cells were isolated from EYFP transgenic mice (*n* = 10) by FACS sorting. CD8+ OT-I and CD4+ OT-II cells were isolated using Dynabeads. 200 µg/ml OVA protein was added to the DC–T cell cocultures. Proliferation of OT-I and OT-II cells was evaluated by CFSE dilution on the FACS. The right shows the mean and SD of three experiments. (C) Presentation to YA26 T cells. Aortic and splenic CD11c^high CD3− CD19− DX5− cells were isolated using FACS sorting and YA26 T cells with Dynabeads. 500 µg/ml CSP was added to the DC–T cell cocultures. Proliferation of CSP-specific TCR transgenic T cells was evaluated by CFSE dilution. The right shows the mean and SD of three experiments. (D) 5 mg OVA was injected i.v. to CD11c-EYFP (*n* = 10) mice. After 20 h, the aortic cell suspensions were prepared and sorted to isolate EYFP+ and EYFP− cells. Spleen EYFP+ and EYFP− cells were also isolated from the mice. The cells were added to OT-1 T cells at ratio of 1:3. After 3 d, T cell proliferation was analyzed by CFSE dilution. This result is representative of two independent experiments.

Because the cross-presentation of OVA to OT-I transgenic T cells is a particularly sensitive system, we next examined another CD8^{+} T cell, YA26. Because the CSP-specific CD8^{+} TCR transgenic mouse is H-2d restricted, we isolated aortic and splenic CD11c^{+} cells from BALB/c or C×B6 F$_1$ mice by FACS sorting. In accordance with a previous study (13), the number of isolated DCs from these mice was ~50% of that seen with C57BL/6 mice. Nonetheless, the CD11c^{+} aortic cells could induce YA26 T cell proliferation with CSP, whereas CD11c^{−} cells could not (Fig. 5 C). Fig. 5 (B and C, right) shows means from three experiments using aortic DCs as effective antigen-presenting cells, including cross-presentation.

We next examined whether the aortic DCs could cross-present blood-borne protein antigen to T cells. 5 mg OVA was injected i.v. and, after 20 h, the aortic EYFP[+] and EYFP^{−} cells were isolated by FACS sorting. Splenic EYFP[high] and EYFP^{−} cells were also isolated in parallel. When the isolated DCs were mixed with OT-1 cells for 3 d, the EYFP[+] aortic DCs effectively induced the proliferation of OT-1 cells (Fig. 5 D), indicating that aortic DCs can take up and cross-present protein antigen from the blood stream. We were struck by the finding that aortic DCs seemed to capture and present OVA better than splenic DCs under our experimental conditions. We suspect that i.v. OVA is not an optimal system to reveal the antigen capture and presenting activity of splenic DCs because OVA can be recognized by mannose receptors that are expressed on liver sinusoidal endothelium (29, 30). If so, aortic DCs may have more ready access to the injected OVA.

The CD11c promoter-EYFP mouse has been valuable for visualizing DCs in situ, including lymphoid organs and lung (22, 31). We now find that the CD11c-EYFP transgenic mouse is valuable for identifying DCs in the aorta. The strong EYFP stain allows for their ready identification in the subintimal space of select regions of the aorta and in all the cardiac valves. Moreover, the EYFP fluoresence can be used to isolate the DCs by cell sorting and to phenotype the cells to show that they express MHC II and other markers of immature DCs.

The aortic subendothelial space is an important site for the initiation of atherosclerosis because proatherogenic LDL particles can be generated in subendothelial spaces by enzymatic or nonenzymatic modifications during hyperlipidemia (32, 33). Our results that DCs are in subintimal space and capture proteins from the blood stream suggest that these cells should also be considered in generating inflammation and even immunity in atherosclerosis–prone areas. DCs, for example, might present lipids to NKT cells leading to cytokine production and cytotoxicity (34), and DCs appear to have a specialized endocytic system in which internalized substrates are not totally catabolized but, instead, peptides are salvaged for presentation to T cells (35).

Importantly, we verify that aortic CD11c^{+} cells are effective antigen-presenting cells, as is characteristic of DCs. DCs capture invading pathogens to generate resistance to infection, and they contribute to immune tolerance, making these cells an important target in studying pathogenesis and prevention of disease (36). Aortic DCs are mainly localized in areas having

turbulent flow including the aortic valve, sinus, lesser curvature of the aortic arch, and openings of arterial branches. In this study, we find that these DCs can effectively cross-present i.v.-injected OVA to T cells. Turbulent flow may allow DCs in the aorta and cardiac valves to capture disease-related pathogens and proteins and present these to T cells.

MATERIALS AND METHODS

Mice. CD11c-EYFP transgenic mice were a gift of M.C. Nussenzweig, N. Anandasabapathy, and J. Idoyaga (The Rockefeller University, New York, NY). We used C57BL/6 (Taconic), BALB/c (Taconic), and C×B6 F$_1$ (Harlan) mice. Mice were maintained under specific pathogen-free conditions and fed a normal mouse diet ad libitum. Mouse protocols were approved by the Institutional Animal Care and Use Committee of The Rockefeller University.

Antibodies and reagents. Antibodies to cell surface markers were CD11c, MHC II, CD31, CD80, CD86, CD1d, CD40, and CD11b (all obtained from BD). Dynabeads were obtained from Invitrogen. Biotinylated antibodies to CD11c and MHC class II were obtained from BD. The tyramide signal amplification kit was obtained from Invitrogen. OVA protein was obtained from the Seikagaku Corporation.

Aortic single cell preparations and flow cytometric analysis. Aortic single cells were prepared using previous methods with minor modifications (16). In brief, after careful removal of the perivascular fat and cardiac muscle tissues, using microscissors under a dissecting microscope, single cell suspensions from aortic segments, including aortic sinus with valve or aortic arch and thoracic aorta, were prepared by incubation with an enzyme mixture containing 450 U/ml collagenase I, 125 U/ml collagenase XI, 60 U/ml hyaluronidase, and 60 U/ml DNase in modified Dulbecco's PBS with calcium and magnesium for 90 min at 37°C with gentle shaking. Splenic single cell suspensions were prepared by incubation with 400 U/ml collagenase D at 37°C for 30 min. After blocking Fc receptors using culture supernatant of 2.4G2 hybridoma, the cells were stained with the indicated fluorochrome-conjugated antibodies. We used a FACS Caliber instrument (BD), and analyzed flow cytometric data with FlowJo software (Tree Star, Inc).

En face immunostaining and confocal microscopic analysis. The aorta was perfused with 4% ice-cold paraformaldehyde in PBS via the left ventricle. After removing perivascular tissues, the segments of aortic sinus, aortic arch, and thoracic aorta were opened longitudinally and further fixed in 4% paraformaldehyde at 4°C for 30 min. After permeabilization using 0.2% Triton X-100, staining for CD11c, MHC II, and CD31 was performed using the Tyramide amplification (TSA) kit (Invitrogen) according to the manufacturer's protocol. To stain DC processes exposed to the vessel lumen, we omitted the permeabilization of aortic segments with 0.2% Triton X-100. After staining, the aortic segments were mounted on glass slides with aqueous mounting medium. For in vivo CD11c staining, 15 µg of biotinylated anti-CD11c antibody was injected i.v. to CD11c-EYFP mice. After 3 h, the aorta was collected and incubated with 3% H$_2$O$_2$ and TSA blocking buffer to remove endogenous peroxidase activity and block nonspecific antibody binding. Then the aorta was incubated with horseradish peroxidase–conjugated streptavidin for 1 h. After washing with PBS, the stained CD11c was visualized using Alexa Fluor 555 tyramide. The confocal images of en face immunostaining were obtained with an inverted laser scanning microscope (510 Meta; Carl Zeiss, Inc.). All confocal sections were taken along the Z axis to visualize all processes from each DC. We also used the Imaris program (Bitplane) to perform three-dimensional reconstitution of the confocal images taken along the Z axis.

Presentation to OVA-specific TCR transgenic T cells. In the case of CD11c-EYFP transgenic mice, the EYFP-positive and –negative cells were isolated from single cell suspensions of aorta and spleen using FACS sorting (FACS Vantage; BD). For nontransgenic B6 mice, aortic CD11c^{+} and CD11c^{−}

cells were isolated using anti-CD11c magnetic beads (Miltenyi Biotech). CD4^{+} or CD8^{+} T cells were isolated from OT-I or OT-II mice (provided by J. Kuroiwa, The Rockefeller University, New York, NY) by excluding B220^{+}, F4/80^{+}, NK1.1^{+}, I-A[b+], and CD4^{+} (for OT-I) or CD8^{+} (for OT-II) cells using anti–rat IgG Dynabeads (Invitrogen). T cells were added to round bottom microtest wells at 30,000/well and mixed with isolated DCs at a DC/T cell ratio of 1:6. OVA protein and peptide were added to the culture at the indicated concentrations. After 4 d for OT-I or 5 d for OT-II, the proliferation of OT-I or OT-II cells was evaluated by CFSE dilution on the FACS. For DC fixation, isolated DCs were incubated with 2% paraformaldehyde for 10 min at room temperature. After washing with PBS, the fixed DCs were incubated in serum-free RPMI1640 medium containing 0.5M DL-lysine for 30 min. After washing twice with culture medium, the fixed DCs were mixed with T cells and incubated at the indicated concentration of peptide or protein.

Cross-presentation to malaria CSP-specific TCR transgenic T cells. The CSP of *Plasmodium yoelii*–specific TCR transgenic mice and the plasmid for the CSP expression have been previously described (37, 38). After induction of CSP expression in *Escherichia coli* (BL-21), His-tagged CSP was isolated using Ni-NTA and then subjected to FPLC to obtain high protein purity without contaminating endotoxin. The protein buffer was then exchanged for serum-free RPMI1640 medium using a Centricon (Millipore). Aortic and splenic CD11c^{high} CD3^{−} CD19^{−} DX5^{−} DCs from C×B6 F$_1$ mice were isolated by FACS sorting. The CSP-specific CFSE-labeled CD8^{+} T cells were negatively selected by excluding B220^{+}, F4/80^{+}, NK1.1^{+}, I-A[d+], and CD4^{+} cells using anti–rat IgG Dynabeads (Invitrogen) and mixed with isolated DCs and antigens including protein and peptide for 4 d as indicated in the results.

In vivo OVA presentation. 5 mg OVA was injected i.v. to CD11c-EYFP mice. After 20 h, the aortic segments were dissociated by enzyme mixture (450 U/ml collagenase I, 125 U/ml collagenase XI, 60 U/ml hyaluronidase, and 60 U/ml DNase), and the EYFP[+] and EYFP^{−} cells were isolated by FACS sorting. The isolated cells were mixed with OT-1 cells at ratio of 1:3. After 3 d, T cell proliferation was analyzed by CFSE dilution.

Online supplemental material. Fig. S1 shows the comparison of cell surface markers of aortic and splenic endogenous CD11c^{+} DCs. Fig. S2 demonstrates that OT-I cells can respond to relatively low doses of OVA presented by splenic DCs when compared with mouse malaria CSP-specific TCR transgenic CD8^{+} T cells. Fig. S3 indicates that the OVA and CSP preparations were not contaminated with active peptides. Fig. S4 shows the importance of DC dose and culture time for cross-presentation. Video 1 shows the subintimal localization of aortic DCs. Video 2 shows that some DCs infrequently have dendritic process extending to aortic lumen. Video 3 shows that the DC processes are localized on the surface of elastic lamina. Online supplemental material is available at http://www.jem.org/cgi/content/full/jem.20082129/DC1.

REFERENCES

1. Johnston, S.L., R.J. Lock, and M.M. Gompels. 2002. Takayasu arteritis: a review. *J. Clin. Pathol.* 55:481–486.

2. Ma-Krupa, W., M. Kwan, J.J. Goronzy, and C.M. Weyand. 2005. Toll-like receptors in giant cell arteritis. *Clin. Immunol.* 115:38–46.

3. Shimizu, K., R.N. Mitchell, and P. Libby. 2006. Inflammation and cellular immune responses in abdominal aortic aneurysms. *Arterioscler. Thromb. Vasc. Biol.* 26:987–994.

4. Hansson, G.K., and P. Libby. 2006. The immune response in atherosclerosis: a double-edged sword. *Nat. Rev. Immunol.* 6:508–519.

5. Steinman, R.M., and H. Hemmi. 2006. Dendritic cells: translating innate to adaptive immunity. *Curr. Top. Microbiol. Immunol.* 311:17–58.

6. Bobryshev, Y.V., and R.S. Lord. 1995. S-100 positive cells in human arterial intima and in atherosclerotic lesions. *Cardiovasc. Res.* 29:689–696.

7. Bobryshev, Y.V., and R.S. Lord. 1999. 55-kD actin-bundling protein (p55) is a specific marker for identifying vascular dendritic cells. *J. Histochem. Cytochem.* 47:1481–1486.

8. Millonig, G., H. Niederegger, W. Rabl, B.W. Hochleitner, D. Hoefer, N. Romani, and G. Wick. 2001. Network of vascular-associated dendritic cells in intima of healthy young individuals. *Arterioscler. Thromb. Vasc. Biol.* 21:503–508.

9. Bobryshev, Y.V., and R.S. Lord. 2002. Expression of heat shock protein-70 by dendritic cells in the arterial intima and its potential significance in atherogenesis. *J. Vasc. Surg.* 35:368–375.

10. Ma-Krupa, W., M.S. Jeon, S. Spoerl, T.F. Tedder, J.J. Goronzy, and C.M. Weyand. 2004. Activation of arterial wall dendritic cells and breakdown of self-tolerance in giant cell arteritis. *J. Exp. Med.* 199:173–183.

11. Pryshchep, O., W. Ma-Krupa, B.R. Younge, J.J. Goronzy, and C.M. Weyand. 2008. Vessel-specific Toll-like receptor profiles in human medium and large arteries. *Circulation.* 118:1276–1284.

12. Bobryshev, Y.V. 2005. Dendritic cells in atherosclerosis: current status of the problem and clinical relevance. *Eur. Heart J.* 26:1700–1704.

13. Jongstra-Bilen, J., M. Haidari, S.N. Zhu, M. Chen, D. Guha, and M.I. Cybulsky. 2006. Low-grade chronic inflammation in regions of the normal mouse arterial intima predisposed to atherosclerosis. *J. Exp. Med.* 203:2073–2084.

14. Mullick, A.E., K. Soldau, W.B. Kiosses, T.A. Bell III, P.S. Tobias, and L.K. Curtiss. 2008. Increased endothelial expression of Toll-like receptor 2 at sites of disturbed blood flow exacerbates early atherogenic events. *J. Exp. Med.* 205:373–383.

15. Liu, P., Y.R. Yu, J.A. Spencer, A.E. Johnson, C.T. Vallanat, A.M. Fong, C. Patterson, and D.D. Patel. 2008. CX3CR1 deficiency impairs dendritic cell accumulation in arterial intima and reduces atherosclerotic burden. *Arterioscler. Thromb. Vasc. Biol.* 28:243–250.

16. Galkina, E., A. Kadl, J. Sanders, D. Varughese, I.J. Sarembock, and K. Ley. 2006. Lymphocyte recruitment into the aortic wall before and during development of atherosclerosis is partially L-selectin dependent. *J. Exp. Med.* 203:1273–1282.

17. Tacke, F., D. Alvarez, T.J. Kaplan, C. Jakubzick, R. Spanbroek, J. Llodra, A. Garin, J. Liu, M. Mack, N. van Rooijen, et al. 2007. Monocyte subsets differentially employ CCR2, CCR5, and CX3CR1 to accumulate within atherosclerotic plaques. *J. Clin. Invest.* 117:185–194.

18. Llodra, J., V. Angeli, J. Liu, E. Trogan, E.A. Fisher, and G.J. Randolph. 2004. Emigration of monocyte-derived cells from atherosclerotic lesions characterizes regressive, but not progressive, plaques. *Proc. Natl. Acad. Sci. USA.* 101:11779–11784.

19. Seo, S.K., J.H. Choi, Y.H. Kim, W.J. Kang, H.Y. Park, J.H. Suh, B.K. Choi, D.S. Vinay, and B.S. Kwon. 2004. 4-1BB-mediated immunotherapy of rheumatoid arthritis. *Nat. Med.* 10:1088–1094.

20. Burt, B.M., G. Plitas, J.A. Stableford, H.M. Nguyen, Z.M. Bamboat, V.G. Pillarisetty, and R.P. Dematteo. 2008. CD11c identifies a subset of murine liver natural killer cells that responds to adenoviral hepatitis. *J. Leukoc. Biol.* 84:1039–1046.

21. Moon, K.A., S.Y. Kim, T.B. Kim, E.S. Yun, C.S. Park, Y.S. Cho, H.B. Moon, and K.Y. Lee. 2007. Allergen-induced CD11b^{+} CD11c^{int} CCR3^{+} macrophages in the lung promote eosinophilic airway inflammation in a mouse asthma model. *Int. Immunol.* 19:1371–1381.

22. Lindquist, R.L., G. Shakhar, D. Dudziak, H. Wardemann, T. Eisenreich, M.L. Dustin, and M.C. Nussenzweig. 2004. Visualizing dendritic cell networks *in vivo. Nat. Immunol.* 5:1243–1250.

23. Skowasch, D., S. Schrempf, N. Wernert, M. Steinmetz, A. Jabs, I. Tuleta, U. Welsch, C.J. Preusse, J.A. Likungu, A. Welz, et al. 2005. Cells of primarily extra-valvular origin in degenerative aortic valves and bioprostheses. *Eur. Heart J.* 26:2576–2580.

24. Grandmougin, D., G. Fayad, D. Moukassa, C. Decoene, K. Abolmaali, J.C. Bodart, M. Limousin, and H. Warembourg. 2000. Cardiac valve papillary fibroelastomas: clinical, histological and immunohistochemical studies and a physiopathogenic hypothesis. *J. Heart Valve Dis.* 9: 832–841.

25. Oei, F.B., A.P. Stegmann, F. van der Ham, P.E. Zondervan, L.M. Vaessen, C.C. Baan, W. Weimar, and A.J. Bogers. 2002. The presence of immune stimulatory cells in fresh and cryopreserved donor aortic and pulmonary valve allografts. *J. Heart Valve Dis.* 11:315–324.

26. Newman, P.J., M.C. Berndt, J. Gorski, G.C. White II, S. Lyman, C. Paddock, and W.A. Muller. 1990. PECAM-1 [CD31] cloning and relation to adhesion molecules of the immunoglobulin gene superfamily. *Science.* 247:1219–1222.

27. Chieppa, M., M. Rescigno, A.Y.C. Huang, and R.N. Germain. 2006. Dynamic imaging of dendritic cell extension into the small bowel lumen in response to epithelial cell TLR engagement. *J. Exp. Med.* 203:2841–2852.

28. Zavala, F., J.P. Tam, P.J. Barr, P.J. Romero, V. Ley, R.S. Nussenzweig, and V. Nussenzweig. 1987. Synthetic peptide vaccine confers protection against murine malaria. *J. Exp. Med.* 166:1591–1596.

29. Hubbard, A.L., G. Wilson, G. Ashwell, and H. Stukenbrok. 1979. An electron microscope autoradiographic study of the carbohydrate recognition systems in rat liver. I. Distribution of ^{125}I-ligands among the liver cell types. *J. Cell Biol.* 83:47–64.

30. Kindberg, G.M., S. Magnusson, T. Berg, and B. Smedsrod. 1990. Receptor-mediated endocytosis of ovalbumin by two carbohydrate-specific receptors in rat liver cells. The intracellular transport of ovalbumin to lysosomes is faster in liver endothelial cells than in parenchymal cells. *Biochem. J.* 270:197–203.

31. Veres, T.Z., S. Rochlitzer, M. Shevchenko, B. Fuchs, F. Prenzler, C. Nassenstein, A. Fischer, L. Welker, O. Holz, M. Muller, et al. 2007. Spatial interactions between dendritic cells and sensory nerves in allergic airway inflammation. *Am. J. Respir. Cell Mol. Biol.* 37:553–561.

32. Oorni, K., and P.T. Kovanen. 2006. Enhanced extracellular lipid accumulation in acidic environments. *Curr. Opin. Lipidol.* 17:534–540.

33. Stocker, R., and J.F. Keaney Jr. 2004. Role of oxidative modifications in atherosclerosis. *Physiol. Rev.* 84:1381–1478.

34. Fujii, S., K. Shimizu, H. Hemmi, and R.M. Steinman. 2007. Innate Valpha14(+) natural killer T cells mature dendritic cells, leading to strong adaptive immunity. *Immunol. Rev.* 220:183–198.

35. Delamarre, L., M. Pack, H. Chang, I. Mellman, and E.S. Trombetta. 2005. Differential lysosomal proteolysis in antigen–presenting cells determines antigen fate. *Science.* 307:1630–1634.

36. Steinman, R.M., and J. Banchereau. 2007. Taking dendritic cells into medicine. *Nature.* 449:419–426.

37. Boscardin, S.B., J.C. Hafalla, R.F. Masilamani, A.O. Kamphorst, H.A. Zebroski, U. Rai, A. Morrot, F. Zavala, R.M. Steinman, R.S. Nussenzweig, and M.C. Nussenzweig. 2006. Antigen targeting to dendritic cells elicits long-lived T cell help for antibody responses. *J. Exp. Med.* 203:599–606.

38. Sano, G., J.C. Hafalla, A. Morrot, R. Abe, J.J. Lafaille, and F. Zavala. 2001. Swift development of protective effector functions in naive CD8^{+} T cells against malaria liver stages. *J. Exp. Med.* 194:173–180.